

The Error Analysis of a Steady-State Thermal Conductivity Measurement Method With Single Constant Temperature Region

Ming-Tsung Sun¹
Chin-Hsiang Chang²

Department of Mechanical Engineering,
Chang Gung University,
259 Wen-Hwa 1st Road,
Kwei-Shan, Tao-Yuan 333, Taiwan

A method for steady-state thermal conductivity measurement with single constant temperature region has been developed. To better understand the accuracy of the method a numerical model is devised and verified by experimental results. The ratios of thermal conductivity derived from the temperature distribution solutions to that given in the numerical model are obtained and shown. They can be used to correct the systematic error of measurement introduced by the one-dimensional approximation. Finally, the measurement uncertainty due to misalignment of the temperature sensors and the limitation of sensing devices is also investigated. The numerical model is suitable for estimating the range of confidence in practical measurements. [DOI: 10.1115/1.2739585]

Keywords: steady-state thermal conductivity measurement, systematic error, measurement uncertainty

1 Introduction

In the applications of the steady-state measurement of thermal conductivity, at least two constant temperature regions are believed to be essential as a heat source and a heat sink, respectively. The constant temperature region as the heat sink requires cumbersome equipment. This limits the use of steady-state measurement methods in laboratories and makes them unsuitable for in situ measurements. In other words, it is hard to apply a steady-state measurement method in a portable apparatus. Extra care has also been taken in the insulation of the apparatus when test samples have small values of thermal conductivity, such as that of the insulation materials. In this case, the destruction of the test sample is inevitable [1]. However, for the composite insulation materials consisting of vacuum layers or glass panels [2], an inverse computational method to evaluate temperature dependence of thermal conductivity [3], or materials with a nonhomogeneous inner structure [4], nondestructive evaluation of the thermal conductivity is required.

In spite of the inconvenience steady-state measurement methods may bring, they are still widely used due to their reliability in measuring composite insulation materials. To fulfill the requirement of nondestructive steady-state measurement of thermal conductivity, Chuah and Sun [5] proposed a method that requires only one constant temperature region as the heat source. A detailed working principle of the method is given by Chuang [6] who devised a microcontroller to perform the automatic measuring procedures. Here, we give only a brief description and show the schematic drawing of the device in Fig. 1.

The method makes use of two electronically controlled heating devices to keep the heating cover and the heating plate at constant temperatures, T_U and T_0 , respectively, on one side of the test

sample. The diameter of the heating cover is D_o and that of the heating plate is D_c . The heating plate is placed inside the heating cover with a small gap, g , inbetween them to avoid direct conduction heat transfer and maintain a larger area of constant temperature. The heating cover is placed inside a stainless-steel housing. The enclosed space between two heating devices and the housing is filled with aerogel.

On the other side of the test sample, a Teflon disk is placed aligned with the heating compartment to hold five temperature sensors. The Teflon disk sizes are D_l in diameter and s in thickness. One of the five temperature sensors is located at the center of the disk and the other four equally spaced on the concentric circle of radius d . They are placed on the side of the disk next to the sample.

Making T_U and T_0 equal, a region of constant temperature can be formed on one side of a test sample. This ensures that the heating power of the heating plate will transmit upward into the test sample only. Since the heat flux moves mostly in the longitudinal direction across the thickness of the test sample, one can achieve effective one-dimensional heat transfer in the measurement. When the temperatures on both sides of the test sample become stable, the temperatures, the thickness of the material, and the heat flux are measured to evaluate the thermal conductivity of the test sample. Using this method, the thermal conductivity of a piece of polystyrene foam was measured and compared with the result using the guarded hot plate method. The relative difference is within 3% [7].

However, due to the multidimensional effect and the temperature distribution on the low-temperature side, the temperature difference used to calculate the thermal conductivity may greatly deviate from that in one-dimensional heat transfer. This situation can be worsened when the sample thickness is larger. Since the systematic variation is inevitable, it is then a good practice to estimate the systematic error of the measured thermal conductivity as a function of the relative sample thickness, H/D_o . The geometric parameter, D_c over D_o , is also considered since it contributes to the systematic error.

As for the random errors, the sources can be the uncertainties of

¹Corresponding author. e-mail: mtsun@mail.cgu.edu.tw

²e-mail: changch@post.savs.ilc.edu.tw

Contributed by the Heat Transfer Division of ASME for publication in the JOURNAL OF HEAT TRANSFER. Manuscript received January 10, 2006; final manuscript received December 14, 2006. Review conducted by A. Haji-Sheikh. Paper presented at the ASME Summer Heat Transfer Conference (HT2003), Las Vegas, NV, USA, July 21–23, 2003.

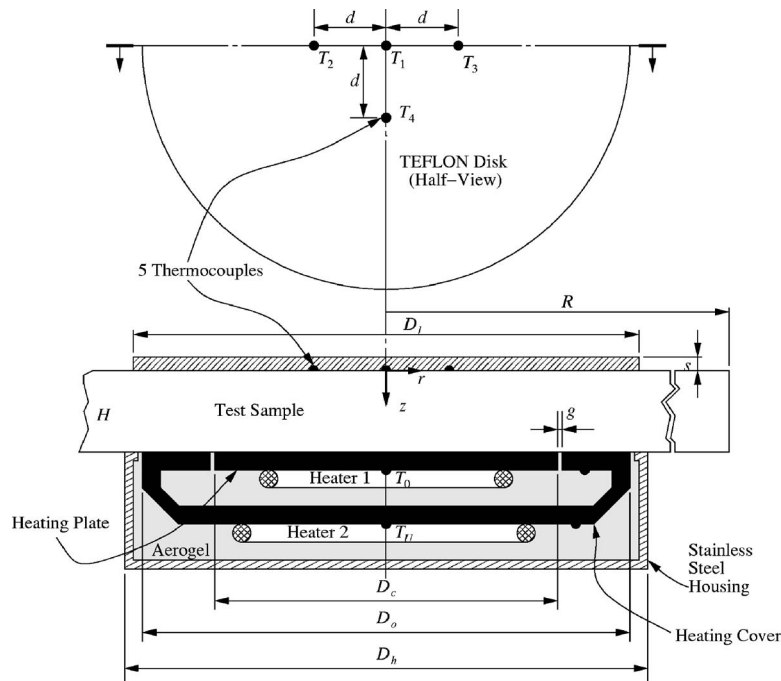


Fig. 1 The descriptive diagram of the device that measures steady-state thermal conductivity.

sensor measurement and imperfect alignment of the five temperature sensors with the heating compartment. They propagate through the formula used for thermal conductivity evaluation. Both systematic and random errors require close investigation before the measurement method can be confidently practiced.

To accomplish the analysis without dealing with the errors caused by insufficiency in the fabrication skill of the experiment apparatus, we established a theoretical model in axial symmetric cylindrical coordinates. The theoretical model is solved numerically because the boundary conditions of free convection are nonlinear and the thermal conductivities of samples are functions of temperature. For nonlinear problems such as the wall effect on hot-wire measurements [8], numerical solutions are often sought. From the model, temperature distribution in the sample can be solved. The heat flux from the heating plate is determined from the solution of temperature distribution since the temperature value is specified on the boundary of the constant temperature region.

With the heat flux and the temperature distribution, the thermal conductivity can be derived from the numerical simulation according to the formula of one-dimensional heat conduction used by the measuring method. This thermal conductivity, denoted as k_E , is different from what is specified in the numerical model, which is denoted as k_R . The ratio of k_E to k_R , the k ratio $r_k = k_E/k_R$, is an indication of measurement deviations from real situations.

By varying the affecting factors, such as H/D_o and D_c/D_o , one can derive a series of k ratios that can be used to correct the measured thermal conductivity in practical applications. Varying D_c/D_o provides information of the device's geometric effect. It will be shown in Sec. 4 that the geometric effect is smaller as D_c/D_o is smaller. However, due to the manufacturing technique it cannot be too small. It is noted that as D_c/D_o decreases, the gap, g , is maintained at a constant value as well as D_o . That is the area of the constant temperature region remains fixed while the area of the heating plate decreases. In this case, the temperature in the gap can be considered uniformly distributed and with the same value as that of the heating plate and the heating cover.

Finally, the thermal conductivity uncertainty is estimated with

the analysis of the error caused by the measurement uncertainty that propagates through the formulation used in the method. In the analysis, an alternative way of determining the maximum temperature on the lower temperature side is proposed. The thermal conductivity uncertainty is expressed as a function of the misalignment of the temperature sensors with the centerline of the heating plate on the lower temperature side.

2 The Experiment

In order to verify the numerical model in this study, an experiment is first carried out. According to the measuring method the thermal conductivity, k_E , is

$$k_E(T_m) = \frac{\dot{Q}H}{A(T_0 - T_{\max})} \quad (1)$$

where T_{\max} is the maximum temperature at the lower temperature side of the test sample and $T_m = (T_0 + T_{\max})/2$ is the mean temperature at which the test sample is supposed to possess k_E .

If the Teflon disk plate is aligned with the heating plate, $T_{\max} = T_1$. Since it is hard to align the two parts in real measurements, Chuah and Sun [5] proposed an approximate function of temperature distribution as follows

$$T(x, y) = c_1x^2 + c_2x + c_3y^2 + c_4y + c_5 \quad (2)$$

where $c_i, i=1 \dots 5$, are five coefficients to be determined with the five known locations of temperature sensors and the temperatures measured from each sensor, respectively. The maximum temperature T_{\max} occurs at the location where the partial derivatives of Eq. (2) with respect to x and y are zero, i.e., $\partial T/\partial x=0$ and $\partial T/\partial y=0$. Substituting the coordinates solved from the set of the two equations into Eq. (2), one can obtain T_{\max} as

$$T_{\max} = c_5 - \left(\frac{c_2^2}{4c_1} + \frac{c_4^2}{4c_3} \right) \quad (3)$$

However, since the geometry of the device is axisymmetric, the temperature distribution can also be described by the following function

Table 1 The readings of the sensors and the derived quantities.

T_1 (°C)	T_2 (°C)	T_3 (°C)	T_4 (°C)	T_5 (°C)	\dot{Q} (W)	T_{\max} (°C)	T_m (°C)
27.18	26.95	27.12	27.08	27.05	0.541	27.22	32.59

$$T(r) = -ar^2 + b = -a[(x - x_0)^2 + (y - y_0)^2] + b \quad (4)$$

The maximum temperature is supposed to occur at (x_0, y_0) . Using least squares fit, one can solve for the unknown parameters a , b , and (x_0, y_0) . In the solutions, b is the maximum temperature, T_{\max} , which can be expressed as

$$T_{\max} = T_1 - \frac{(T_2 - T_3)^2 + (T_4 - T_5)^2}{4(T_2 + T_3 + T_4 + T_5 - 4T_1)} \quad (5)$$

where T_1 is measured from the central sensor; T_2 and T_3 are measured from the sensors aligned with the center; and T_4 and T_5 are measured likewise but in the perpendicular direction. This form of temperature distribution is much simpler than Eq. (2) because there is no need to solve any coefficients.

The geometry of the experimental device has the following dimensions: $D_o=218$ mm, $H=29$ mm, $D_c=185$ mm, $R=240$ mm, $D_l=200$ mm, $d=40$ mm, and $s=6$ mm. The configuration of experimental device used is in the upsidedown position of that shown in Fig. 1. The constant temperature region is controlled at $T_0=40^\circ\text{C}$. The test sample we use in the experiment is a piece of expanded polystyrene type XI (EPS) thermal foam board.

Due to the quality of the heater controllers, the temperature of the heating plate can only be maintained at 37.95°C . The ambient air temperature, T_a , is 23.35°C . When all the readings are stable for at least 30 min, they are recorded in Table 1. T_{\max} is evaluated from T_1 to T_5 using Eq. (5). Substituting the measurement data into Eq. (1), we have 0.0544 W/m K as the k_E of the test sample evaluated at $T_m=32.59^\circ\text{C}$.

3 The Numerical Model

The numerical model used in this study is based on the heat conduction equation in cylindrical coordinates. Since the device is axially symmetric, we only need to consider a two-dimensional problem. The governing equation is

$$\rho c \frac{\partial T}{\partial t} = \frac{k_r}{r} \frac{\partial}{\partial r} \left(r \frac{\partial T}{\partial r} \right) + k_z \frac{\partial^2 T}{\partial z^2} \quad (6)$$

where ρ and c are the density and heat capacity of the material under testing. To simplify the problem, we first assume that the test sample has a constant c and isotropic k , i.e., $k_r=k_z$. The isotropic k value of the test sample (EPS foam of ASTM designation type XI) is a function of temperature as

$$k = 0.000163 \times T + 0.04265 \quad (7)$$

where temperature T is in $^\circ\text{C}$ and k is in W/m K. This formula is derived by linear regression of the data provided by Thermal Foams, Inc. The thermal conductivity of the Teflon disk plate is also a function of temperature [9] as

$$k = 0.001 \times T + 0.323 \quad (8)$$

where the units are the same as those in Eq. (7).

The boundary conditions of the numerical model are summarized in Table 2 where the origin of the coordinates is at the center of the Teflon disk plate on the inner surface (as shown in Fig. 1).

One may argue that the heat transfer across the interface of two contact surfaces depends on the profile of the surfaces as in the studies of many, such as Wahid et al. [10–12]. In our model, the interfaces locate at the two sides of the test sample in contact with the heating plate and the Teflon disk plate. As a matter of fact, if the k value of the test sample is as small as in our case, the contact

surface effect can be ignored. However, for large k values, dissipative jelly can be applied at the interfaces to fill the voids and minimize the contact surface effect of the interface air layer. Therefore, we ignore the effect in our model with the assumption that one should use dissipative jelly in the practical applications of the method for measuring the materials of large k value.

As mentioned before, the coefficient of free convection on each boundary is nonlinear. In this study, we use the empirical formulation of convection coefficient given by Janna [13]. For the vertical surfaces, the formulation is

$$h_{L,V} = \frac{k_f}{L} \times \left\{ 0.825 + \frac{0.387 \text{Ra}_{L_C}^{1/6}}{\left[1 + \left(\frac{0.492}{\text{Pr}} \right)^{9/16} \right]^{8/27}} \right\}^2 \quad (9)$$

where the unit of convection coefficient is W/m² K. For the lower surfaces, the convection coefficient is

$$h_{L,H_l} = \frac{k_f}{L} \times 0.27 \text{Ra}_{L_C}^{1/4} \quad (10)$$

For the upper surfaces of the test sample, depending on the range of Rayleigh number the coefficient are given as

$$h_{L,H_u} = \frac{k_f}{L} \times 0.54 \text{Ra}_{L_C}^{1/4}, \quad 2.6 \times 10^4 < \text{Ra}_{L_C} < 10^7$$

$$h_{L,H_u} = \frac{k_f}{L} \times 0.15 \text{Ra}_{L_C}^{1/3}, \quad 10^7 < \text{Ra}_{L_C} < 3 \times 10^{10} \quad (11)$$

In Eqs. (9)–(11), k_f is the thermal conductivity of the fluid, which is air in our case; Ra_{L_C} is the Rayleigh number based on the characteristic length L_C ; Pr is the Prandtl number of the air; and L is the width of the surface.

Since the measuring method is done under steady-state measurement, the time varying term on the left-hand side of Eq. (6) equals zero. The successive over relaxation (SOR) method is chosen due to its wide use in parabolic problems. The acceptance criterion of a convergent solution is that the maximum relative variation of temperature in the model is less than 10^{-9} . Asymptotic tests are done first to determine the maximum grid sizes and the minimum radius of the test sample in the numerical model.

After the temperature distribution in the numerical model is solved, the measuring process is simulated by first acquiring temperatures, T_i , at the locations of the five temperature sensors (i

Table 2 The boundary conditions of the model.

r coordinate	z coordinate	B.C. description
$r=0$	$-s \leq z \leq H$	Axial symmetric
$r=R$	$0 \leq z \leq H$	Free conv. ^a ($h_{L,V}$)
$0 < r \leq D_o/2$	$z=H$	Isothermal ($T=T_0$)
$D_o/2 < r \leq R$	$z=H$	Free conv. ^b (h_{L,H_l})
$0 < r \leq D_l/2$	$z=-s$	Free conv. ^c (h_{L,H_u})
$r=D_l/2$	$-s < z \leq 0$	Free conv. ^a ($h_{L,V}$)
$D_l/2 < r \leq R$	$z=0$	Free conv. ^c (h_{L,H_u})

^aEquation (9) on vertical walls.

^bEquation (10) on horizontal walls facing downward.

^cEquation (11) on horizontal walls facing upward.

= 1, 2, 3, 4, 5) and the heat transfer rate of the heating plate, \dot{Q} , out of the heating plate into the test sample. T_{\max} can be determined according to Eq. (5). The heat transfer rate, \dot{Q} , which is supposed to be the power of the heater on the heating plate, is evaluated as by

$$\begin{aligned} \dot{Q} = 2\pi \left\{ \sum_{i=1}^m r_i \times \Delta r_i \times k \left(\frac{T_{i,n} + T_{i,n-1}}{2} \right) \times \frac{T_{i,n} - T_{i,n-1}}{z_n - z_{n-1}} + \sum_{j=n+1}^N \left(r_m \right. \right. \\ \left. \left. + \frac{\Delta r_m}{2} \right) \times \left[\Delta z_j \times k \left(\frac{T_{m,j} + T_{m+1,j}}{2} \right) \times \frac{T_{m,j} - T_{m+1,j}}{r_{m+1} - r_m} + \frac{\Delta z_N}{2} \right. \right. \\ \left. \left. \times k \left(\frac{3T_{m,N} + T_{m,N-1} + 3T_{m+1,N} + T_{m+1,N-1}}{8} \right) \right. \right. \\ \left. \left. \times \frac{3T_{m,N} + T_{m,N-1} - 3T_{m+1,N} - T_{m+1,N-1}}{4(r_{m+1} - r_m)} \right] \right\} \quad (12) \end{aligned}$$

where z_N locates at the interface between the heating plate and the test sample; $r_m + \Delta r_m/2$ locates at the rim of the heating plate; and $(z_n + z_{n-1})/2$ is the surface where we integrate the heat flux in the z direction. With the resulting \dot{Q} and T_{\max} , and the known variables in the model T_0 , $A = (\pi D_c^2)/4$, and H , the k_E from the numerically simulating measurement, can be determined using Eq. (1). This k_E is then divided by $k_R = k(T_m)$ evaluated with Eq. (7) to give the k ratio for the given parameters.

To analyze the random error of the measurement, we have to consider the error from temperature measurement, temperature control, and the heating power readout that propagate to generate uncertainty in the measured thermal conductivity δk_E . The relative uncertainty of the measured thermal conductivity u_{k_E} can be expressed as

$$u_{k_E} \equiv \frac{\delta k_E}{k_E} = \left\{ \left(\frac{\delta \dot{Q}}{\dot{Q}} \right)^2 + \left(\frac{\delta T_0}{T_0 - T_{\max}} \right)^2 + \left(\frac{T_{\max}}{T_0 - T_{\max}} \frac{\delta T_{\max}}{T_{\max}} \right)^2 \right\}^{1/2} \quad (13)$$

In the equation, both the measurement error and the offset of the temperature sensors that propagate through the temperature distribution function contribute to $\delta T_{\max}/T_{\max}$. The situation of the offset temperature sensors is simulated by finding the temperature of each sensor from the numerical solution of temperature distribution on the lower temperature side of the sample with the desired offset amount.

4 Results and Discussions

In verifying the numerical model, the numerical model is built according to the setups of the experiment. Except for the constant temperature region, the temperature distribution on the contact surface between the sample and the housing is considered. The temperature in between D_o and D_h is specified with linear distribution from T_0 to T_a , which is very close to the real situation.

With the parameters specified in the experiment, the asymptotic tests for the model give the results of 36 longitudinal nodes and 241 radial nodes for the computational domain. The temperature at the monitoring location where T_1 is measured has a relative variation of less than 10^{-4} when the node numbers increase further.

The results of the simulation are listed in the first row of Table 3 in which T_2 – T_5 are not listed and are the same due to axial symmetric and aligned Teflon disk assumptions. Compared with the experimental results, although there is at most 3% difference for all the quantities, the calculated k_E using Eq. (1) is also 0.0544 W/m K. By this, the numerical model is verified.

In order to see the effect of convection coefficients, the convection coefficients from Eqs. (9)–(11) are multiplied with a h factor and used in the numerical model. The results are shown in the

Table 3 The simulation results.

h factor	T_1 (°C)	\dot{Q} (W)	T_{\max} (°C)	T_m (°C)	k_E (W/m K)
1.0	27.68	0.524	27.68	32.82	0.0544
1.2	27.29	0.540	27.29	32.62	0.0540

second row of Table 3 and indicate that although the convection coefficients increase by 20%, the predicted k_E varies by less than 1%. This shows that the measuring method is insensitive to the conditions of the environment. It is interesting to note from the results that the simulated T_1 and \dot{Q} with the 1.2 h factor are much closer to the experimental ones. Therefore, Janna's formulation may not be able to apply directly in this case. Therefore, the 1.2 h factor is used in the following simulations for error analysis.

To analyze the systematic error of the measuring method, the relative thickness of the test sample, H/D_o , and the relative diameter of the heating plate, D_c/D_o , are varied in the numerical model. The k ratios resulting from the numerical model are shown in Fig. 2 with solid symbols, in which the case of the experiment is indicated by an arrow.

In Fig. 2, it is expected that as the thickness of the sample and the area of the heating decrease relative to the unchanged constant temperature area, the situation of ideal one-dimensional heat conduction can be better approximated. Also, since the radial heat flux always makes the heating power of the heating plate larger than what actually penetrates the sample, it consequently introduces a larger k value. That is, the k ratios of this measurement method are always greater than unity.

However, the k ratio values do not approach unity when the relative thickness of the sample approaches zero. This is caused by the discontinuity of the thermal effusivity, which locates at the edge of the Teflon disk and is near the rim of the heating cover. As shown in Fig. 3, the discontinuity of thermal effusivity at D_l contributes to the jag of the temperature distribution. The location is near D_c , which is the outer boundary of \dot{Q} considered for calculating the k value. When the sample thickness is small, \dot{Q} is still overestimated since the heat flux is greater in regions not covered by the Teflon disk. To further show this, the discontinuity of the thermal effusivity is moved away from the rim of the heating plate, that is, the size of the Teflon disk is enlarged up to the size where there is no more change to the resulting k ratios. The final dimension of the disk is 400 mm in diameter with the associated ratio $D_l/D_o = 1.84$, which is twice the original size. The k ratios obtained with the new model are also shown in Fig. 2 using open symbols. The k ratios of the same D_c/D_o are smaller than before and approach unity when the relative thickness approaches zero.

Yet, the values of the k ratio are quite large. It is interesting to see the effect of the temperature distribution outside the constant temperature region. To do so, the temperature varying boundary condition is removed and the values of the k ratio turn out to be about half of the previous results. They are shown in Fig. 4 with a different vertical scale. The effect of the rim is much more obvious in this case for both the value differences and the shape of the curves.

In addition to isotropic materials, an anisotropic material is modeled such that its thermal conductivity in the radial direction is three times that in the longitudinal direction, i.e., $k_r = 3k_z$. The resulting k ratios are so close to that of an isotropic material that they overlap in the figure and are needless to show in the paper. This result may suggest that the measurement method is insensitive to the type of material under testing, at least for any composite material whose effective thermal conductivities in two directions are related by a proportional factor only.

As for the uncertainty of the measured thermal conductivity caused by the measurement uncertainties of the temperature read-

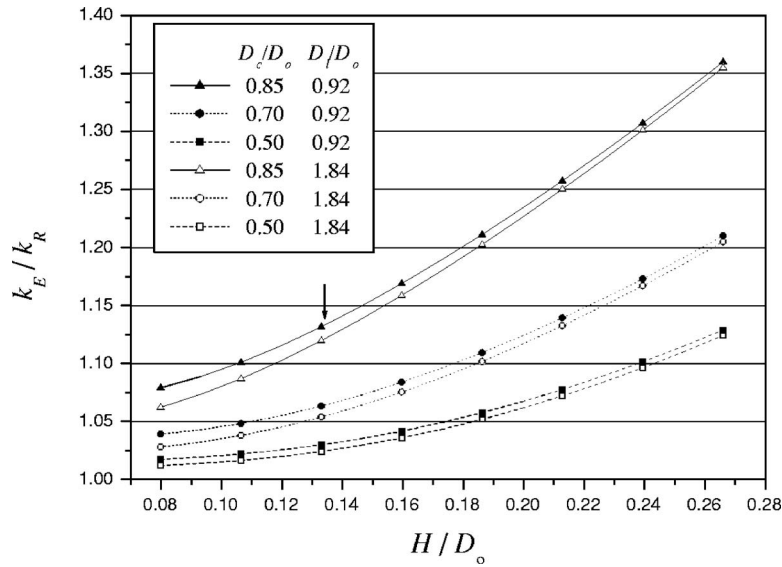


Fig. 2 The k ratio derived from different geometric parameters.

ings, the temperature control, the heating power reading, and the misalignment of the Teflon disk is inspected. The measurement uncertainties considered in our case are $\pm 0.5^\circ\text{C}$ (ΔT_i) for temperature measurement (considering a random error of $\pm 0.4^\circ\text{C}$ from NIST certified standard for a T-type thermocouple and a bias error of $\pm 0.3^\circ\text{C}$), $\pm 0.0195\text{ W}$ ($\Delta \dot{Q}$) (using a 10 W heater with an 8-bit resolution pulse width modulation (PWM) controller) for the power readout, $\pm 0.5^\circ\text{C}$ (ΔT_0) for constant temperature control, and d for both x_{offset} and y_{offset} .

In the analysis, both the approximate temperature distribution functions, Eqs. (2) and (4), on the lower temperature surface of a test sample are considered. Equation (13) gives us an estimation of relative uncertainty of measured k shown in Fig. 5. In the figure, the left panel is the uncertainty estimated using Eq. (3) to evaluate T_{max} while the right panel is that using Eq. (5). On the left panel, u_{k_E} varies axisymmetrically in the range from 0.08939 to 0.13795. On the right panel, u_{k_E} varies more or less axisymmetrically in the range from 0.08965 to 0.10353. Comparing the

two panels, one can see that using Eq. (5) to evaluate T_{max} introduces less error than using Eq. (3) with the same amount of misalignment.

The reason for this is more mathematical than physical. Equations (3) and (5) have the same highest order (second order) of spatial coordinate, which is high enough to describe the relatively flat distribution shown in Fig. 3 for $r < d$. However, with five temperature sensors, Eq. (3) is the highest-order function one can use. It cannot tolerate the slightest measurement uncertainty since five known temperature values determine only five unknown coefficients. Nonetheless, with Eq. (5), the measurement uncertainty of each temperature is allowed since the least-squared-fit method is used to solve the four unknowns and has a degree of freedom of 1 ($5-4$). If a function of higher-order polynomial is used, the degree of freedom is reduced. Consequently, the approximated function tolerates less measurement uncertainty.

In order to observe the effect of measurement uncertainties on u_{k_E} , the uncertainties are varied with the use of both equations to

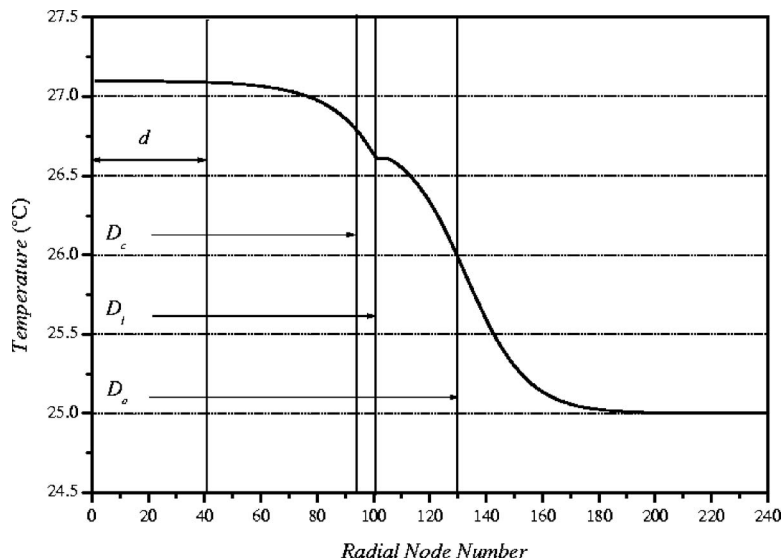


Fig. 3 The temperature distribution on the lower temperature side of a sample.

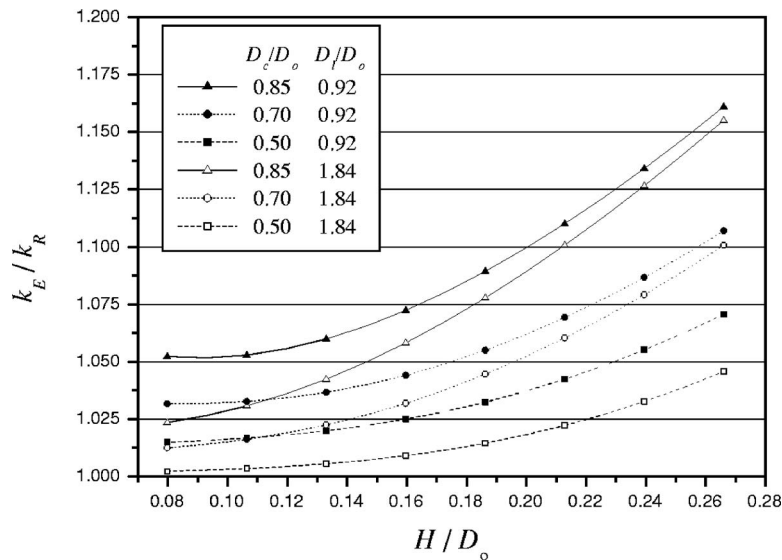


Fig. 4 The k ratio derived without temperature distribution outside the constant temperature region.

evaluate T_{\max} . In Fig. 6, the results in Fig. 5 are repeated as Line 1 and 2 for the left and right panel, respectively, expressed as the functions of radial offset, r_{offset} . If the measurement uncertainties can be lower, such as $\Delta\dot{Q} = \pm 0.00122$ W (using a 10 W heater with a 12-bit resolution PWM controller), the measurement uncertainties ΔT_i and ΔT_0 being the same as $\pm 0.5^\circ\text{C}$, the values of u_{k_E} reduce significantly and are shown as Lines 3 and 4, respectively. It is noted that the tendency of variation in u_{k_E} with respect to r_{offset} is independent of the measurement uncertainties.

5 Conclusion

The numerical model for error analysis of the steady-state thermal conductivity measurement method is established. It is verified by an experiment on a piece of EPS with a prototype measurement device. This model is capable of estimating both systematic and random error of measurements. With the numerical model, systematic errors are derived as correction factors (k ratios) to improve measurement accuracy in practical applications.

In this study, it is found that the diameter of the Teflon disk

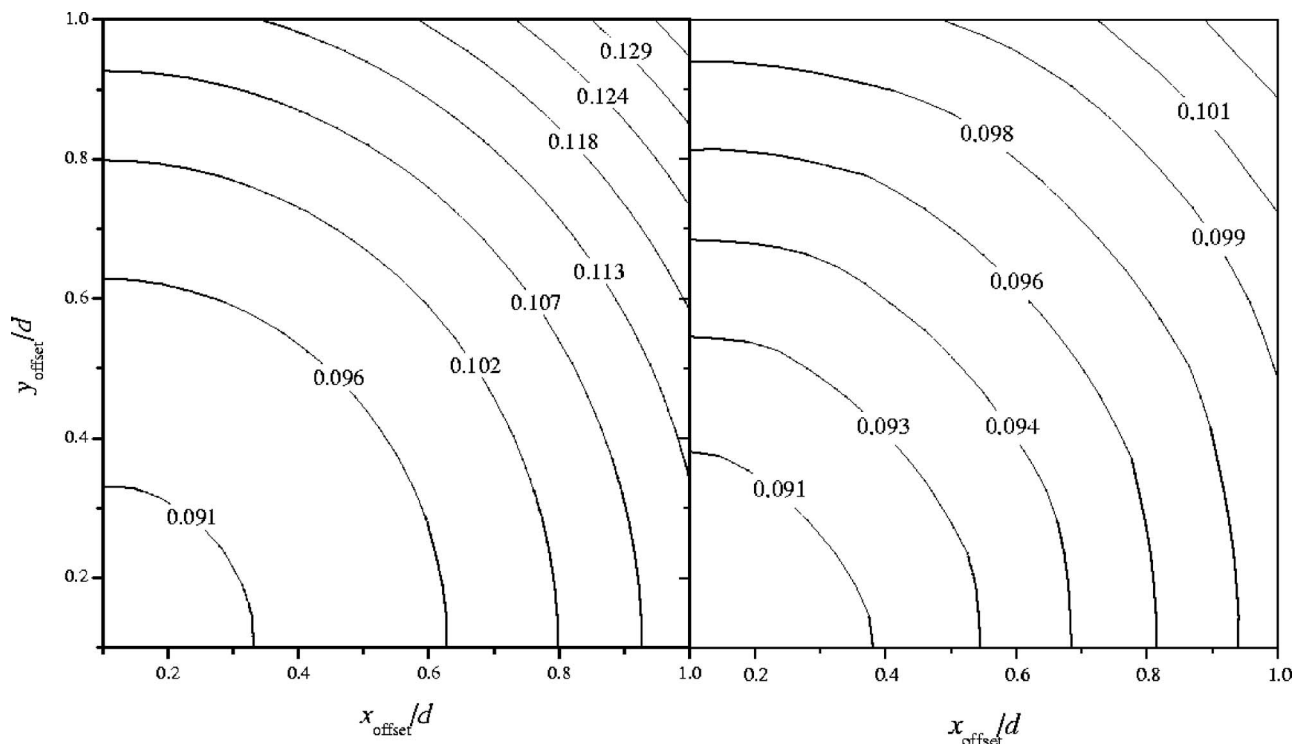


Fig. 5 The relative uncertainty of k_E caused by the uncertainties of measurement and the offset of temperature sensors embedded in the Teflon disk plate using both Eq. (2) (left panel) and Eq. (4) (right panel) to evaluate T_{\max} .

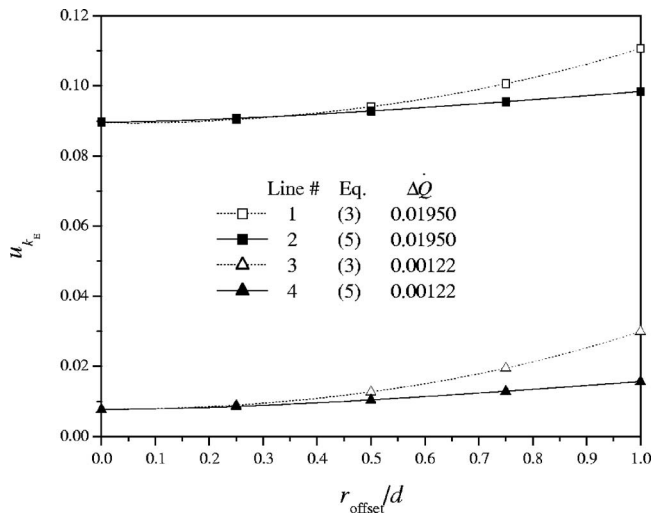


Fig. 6 The relative uncertainty of k_E caused by the uncertainties of measurement and the offset of temperature sensors in the radial direction.

plate, D_l , should be larger than two times D_o to minimize the systematic error. If one wishes to lower the systematic error further, the housing outside the constant temperature area should not contact with the test sample. It is also realized that the measurement method is insensitive to composite materials whose effective thermal conductivities in two directions are related to a proportional factor only. Furthermore, the use of approximate temperature distribution function, Eq. (4), can better describe the actual situation and keep minimal the random error introduced by the misalignment of temperature sensors. This shows that the goal of using an approximate temperature distribution function for k measurement is achieved. The random error in k measurement strongly depends on the uncertainties of the heating power, measuring temperature, and the misalignment of temperature sensors on the lower temperature side.

Referring to Fig. 4, by choosing proper geometric parameters, for example, $D_c/D_o=0.5$ and $D_l/D_o=1.84$, the systematic error can be kept under 5% within a considerable range of sample thickness, $H/D_o < 0.27$. Therefore, the measurement method is considered to be an affordable method due to its simplicity.

However, for more accurate measurements, the systematic error has to be taken into account. But the systematic error also depends on the mean temperature, the ambient temperature, and the k value of the test samples. Though the systematic error can be expressed as an empirical function of geometric parameters and temperatures, it is almost impossible to make the function in a closed form due to its dependency on the unknown itself. Therefore, it is necessary to perform a large number of calculations with this numerical model and generate an equal amount of results. By using an optimization method, such as artificial neuro networks, together with the results, it is possible to seek a calibrating function for real applications of the measurement method.

Acknowledgment

This work was supported by NSC of Taiwan under Grant No. NSC-95-2119-M-182-001.

Nomenclature

- a = coefficient of the alternative approximation temperature distribution function
- A = area of the heating plate, m^2
- b = coefficient of the alternative approximation temperature distribution function

- c_i = coefficients of the original approximation temperature distribution function
- d = distance of the four temperature sensors from the center, m
- D_c = diameter of the heating plate, m
- D_h = diameter of the housing, m
- D_o = diameter of the constant temperature region, m
- D_l = diameter of the Teflon plate, m
- h_{L,H_l} = coefficient of free convection on a horizontal lower surface of width L , $W/m^2 K$
- h_{L,H_u} = coefficient of free convection on a horizontal upper surface of width L , $W/m^2 K$
- $h_{L,V}$ = coefficient of free convection on a vertical surface of width L , $W/m^2 K$
- H = thickness of a test sample, m
- k = thermal conductivity of a homogeneous material, $W/m K$
- k_f = thermal conductivity of the ambient fluid (air), $W/m K$
- k_r = translational thermal conductivity of a composite material, $W/m K$
- k_z = longitudinal thermal conductivity of a composite material, $W/m K$
- k_E = measured thermal conductivity of a test sample, $W/m K$
- k_R = real thermal conductivity of the test sample, $W/m K$
- L = width of a boundary surface of free convection, m
- L_C = characteristic length of a free convection surface, m
- Pr = Prandtl number of the air
- \dot{Q} = heat transfer rate of the heating plate, W
- r = radial coordinate, m
- r_k = k ratio
- R = maximum radius of the test sample in the numerical model, m
- Ra_{L_C} = Rayleigh number based on L_C
- s = thickness of the Teflon disk plate, m
- T_0 = temperature of the constant temperature region, $^{\circ}C$
- T_a = ambient air temperature, $^{\circ}C$
- T_c = temperature at the center of the lower temperature surface, $^{\circ}C$
- T_{max} = maximum temperature on the sample surface opposite to the constant temperature region, $^{\circ}C$
- T_m = mean temperature of T_0 and T_{max} , $^{\circ}C$
- u_{k_E} = relative uncertainty of measured thermal conductivity, k_E
- x_0, y_0 = location of maximum temperature relative to the center of the Teflon disk plate, m
- z = longitudinal coordinate, m
- Δr = radial grid size, m
- Δz = longitudinal grid size, m

References

- [1] Caps, R., Heinemann, U., Fricke, J., and Keller, K., 1997, "Thermal Conductivity of Polyimide Foams," *Int. J. Heat Mass Transfer*, **40**, pp. 269–280.
- [2] Collins, R. E., Fisher-Cripps, A. C., and Tang, J. Z., 1992, "Transparent Evacuated Insulation," *Sol. Energy*, **49**(3), pp. 333–350.
- [3] Martin, T. J., and Dulikravich, G., 2000, "Inverse Determination of Temperature-Dependent Thermal Conductivity Using Steady Surface Data on Arbitrary Objects," *ASME J. Heat Transfer*, **122**, pp. 450–459.
- [4] Herwig, H. and Beckert, K., 2000, "Fourier Versus Non-Fourier Heat Conduction in Materials With a Nonhomogeneous Inner Structure," *ASME J. Heat Transfer*, **122**, pp. 363–365.
- [5] Chuah, Y. K., and Sun, M. T., 1997, "Research on Insulation Testing and Vacuum Insulation Technology (2)," National Council of Science, Taiwan, Report on Supported Research Project (in Chinese), pp. 8–10.
- [6] Chuang, C. C., 1998, "Application of Micro-controller on the Development of

- Heat Transfer Coefficient Measurement Instrument,” Master’s thesis, Chang-Gung University, Taoyuan, Taiwan (in Chinese), pp. 12–14.
- [7] Sun, M. T., Chang, C. H., Chuang, C. C., and Chuah, Y. K., 2002, “A Portable Apparatus with One Constant Temperature Zone for Thermal Conductivity Measurement,” *Proceedings 26th Conference on Theoretical and Applied Mechanics*, Hu-Wei, Taiwan, December 20–21, pp. A049.1-2.
- [8] Shi, J.-M., Breuer, M., Durst, F., and Schafer, M., 2003, “An Improved Numerical Study of the Wall Effect on Hot-Wire Measurements,” *ASME J. Heat Transfer*, **125**, pp. 595–603.
- [9] Incropera, F. P., and DeWitt, D. P., 2001, *Fundamentals of Heat and Mass Transfer*, 5th ed., Wiley, New York, pp. A14–A15.
- [10] Wahid, S. M. S., Madhusudana, C. V., and Leonardi, E., 1998, “An Investigation of the Effect of Gases on Thermal Gap Conductance at Low Contact Pressure,” *Proceedings of 11th International Heat Transfer Conference*, **7**, Kyongju, Korea, August 23–28, Taylor & Francis, Philadelphia, PA, pp. 95–100.
- [11] Wahid, S. M. S., 2003, “Numerical Analysis of Heat Flow in Contact Heat Transfer,” *Int. J. Heat Mass Transfer*, **46**, pp. 4751–4754.
- [12] Wahid, S. M. S., and Madhusudana, C. V., 2003, “Thermal Contact Conductance: Effect of Overloading and Load Cycling,” *Int. J. Heat Mass Transfer*, **46**, pp. 4139–4143.
- [13] Janna, W. S., 1986, *Engineering Heat Transfer*, PWS Publishers, Boston, pp. 533–539.